

smaller and an indication that the idler is being generated in the PhCWG, where there is a much higher GVD. In addition to this bandwidth reduction, the decaying oscillatory peaks of Eq. (1) are resolved in the experimental data of Fig. 3(a) and 3(c). If there was a strong detuning independent (over the ± 5 nm detuning examined here) idler being generated in the channel waveguides it would be expected these oscillations would be washed out and unable to be resolved.

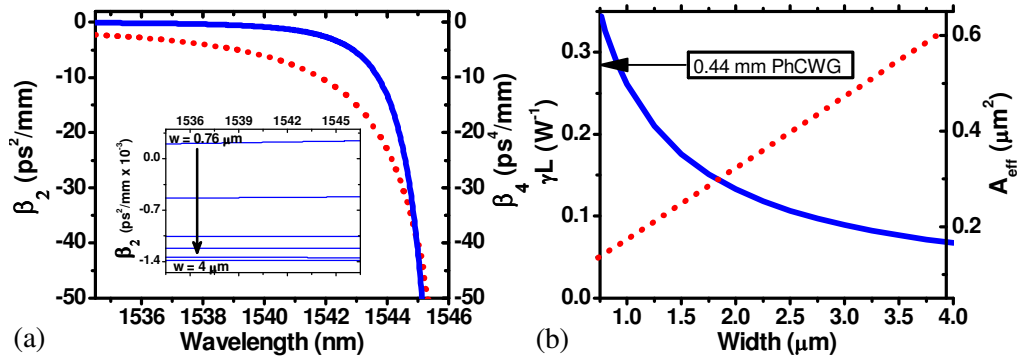


Fig. 4. (a) β_2 (solid line) and β_4 (dotted line) for the photonic crystal waveguide used in this experiment (inset) β_2 for conventional silicon waveguides for various widths (0.76 μm , 1.0 μm , 1.5 μm , 2.0 μm , 3.0 μm , and 4.0 μm) (b) Calculated γL value (solid line) and the A_{eff} (dotted line) versus waveguide width. Arrow indicates the expected minimum ($\lambda_{\text{pump}} = 1535$) value of γ^*L for a 0.44 mm PhCWG (channel waveguide length = 2.1 mm, height = 0.25 μm)

In addition to the observed bandwidth contraction, the measured idler power is observed to increase as the pump wavelength approaches λ_c for fixed pump and signal powers, a telling sign of group index enhancement of the nonlinear parameter. Especially when one considers that the transmission of the waveguide experiences a 5dB drop in transmission between these two wavelengths. In order to justify that the 0.44 mm long PhCWG by itself is responsible we compare it to a theoretical 2.1 mm (the total length of the device minus the length of the PhCWG) long channel waveguide by plotting the $\gamma L = \omega_{\text{pump}} n_2 / c A_{\text{eff}}$ parameter value for a for widths within the range of the taper used in our device, as well as the minimum γ^*L value expected from the 0.44 mm PhCWG. The 0.44 mm long PhCWG shows a larger nonlinear response than the majority of the 2.1 mm long waveguides with widths experienced in the tapered. It is only overtaken by the conventional waveguides when their effective area becomes small enough to compensate for the group index enhancement in the PhCWG. However, the effective area of the conventional waveguide remains relatively constant over the wavelengths investigated here while the PhCWG sees an eight fold increase in group index. Therefore the pump wavelength dependence of the channel waveguides nonlinear parameter can be expected to be flat over the wavelengths examined, while the PhCWGs nonlinear parameter is expected to scale with the square of the group index. Additionally, the actual input/output channel waveguides used in the experiment have a linear taper in width going from the minimum of 0.76 μm to the maximum of 4 μm , therefore a more realistic value we should compare to would be the average γL value of the widths, which is ~ 14 and is half the minimum value expected from the PhCWG. Of course this simple comparison ignores the losses incurred from the PhCWG that occurs between the two channel waveguides in the actual experimental device, which if considered would further show that the idler power measured in the experiment is generated primarily within the PhCWG.

4. Results

In order to quantify the FWM process in the PhCWG, the measured idler powers should be normalized with respect to the coupled signal power in order to gauge the conversion efficiency. The conversion efficiency is derived experimentally by taking the ratio of the measured output idler power and measured output signal power ($\eta P_{idler}^{out} / \eta P_{signal}^{out}$) in order to cancel any uncertainty in the coupling efficiency. It has recently been demonstrated [46] that using this definition can inadvertently overestimate conversion efficiency in silicon channel waveguides due to loss experienced by the signal within the waveguide, either through conventional linear propagation loss or by nonlinear loss due to two-photon and free-carrier absorption. In order to avoid this, the conversion efficiency can be defined as $P_{idler}^{out} / P_{signal}^{in}$. Using this definition the maximum conversion efficiency of our waveguide for this pump power is derived from the maximum measured idler power $\max(\eta P_{idler}^{out}) = -35.6$ dBm, (see Fig. 3(d)) and knowing that P_{signal}^{in} is +11.5 dBm and that the coupling loss is estimated to be 8.5 dB a maximum measured conversion efficiency of -38.8 dB is found. We can conclude that this value is the lower bound estimate of the maximum conversion efficiency of our waveguide for this coupled pump power. The assumption made with this definition is that the coupling to the waveguide of both the pump and signal is wavelength independent, which is valid for channel waveguides for the bandwidths considered here but not for a photonic crystal waveguide which exhibits increased coupling losses as the group index of the PhCWG mode increases.

With the lower bound conversion efficiency of the experiment stated, we will now present the results for the conventional definition ($\eta P_{idler}^{out} / \eta P_{signal}^{out}$) (where ηP_{signal}^{out} is measured with the pump off), in order to make an attempt at correcting for this group index dependent coupling loss. In order for this definition to be valid the conversion efficiencies will be derived from the maximum idler power generated by a signal detuned ± 0.1 nm from the pump wavelength in order to minimize any difference in the group index dependent coupling loss experienced by the idler and signal. The pump wavelength dependence of this conversion efficiency is plotted in Fig. 5(a). The maximum measured conversion efficiency, using the ($\eta P_{idler}^{out} / \eta P_{signal}^{out}$) definition, is -35.7 dB; a difference of ~3 dB compared with the lower bound. This difference stems from the fact that the assumption that the idler and signal are experiencing equivalent coupling and propagation losses begins to break down at large group indices. For these pump wavelengths the maximum generated idler occurs when the signal is red shifted from the pump and consequently experiencing a higher group index and higher losses. This artificial increase in conversion efficiency could be mitigated by reducing the wavelength separation between the pump and signal however we are limited by our filter bandwidths and OSA resolution. In order to explicitly display that the increase in the group index is responsible for the enhancement of the conversion efficiency it is plotted versus group index in Fig. 5(b). In plotting the experimentally measured conversion efficiency, the measured group index is used (red points in Fig. 1(a)) and the wavelength shifted numerically computed group index is used to plot the model conversion efficiency.

The numerical model appears to underestimate the maximum conversion efficiency by 5 dB, which would appear counterintuitive since the simulation does not take into account the decrease in the amount of pump power coupling into the waveguide as the group index increases. It would be expected that because of this fact the numerical model should show higher maximum conversion efficiencies than the experiment. This discrepancy can be attributed to the fact that this simple numerical model does not account for the effect the finite size of the PhCWG has on its transmission, which is responsible for the increasing strength and frequency of the Fabry-Perot oscillations as the cutoff wavelength is approached [18]. A

decrease in the pump and signal wavelength step sizes ($\Delta\lambda_{\text{signal}}$, $\Delta\lambda_{\text{pump}}$) would be expected to reveal the measured data points oscillating about a trend more in line with what is expected. The strength of the Fabry-Perot oscillations can be reduced through proper impedance matching of the channel waveguide and the PhCWG [48]. The high resolution data would also make it possible to accurately probe the dispersion and observe the wavelength/group index at which point disorder can no longer be considered perturbative [49].

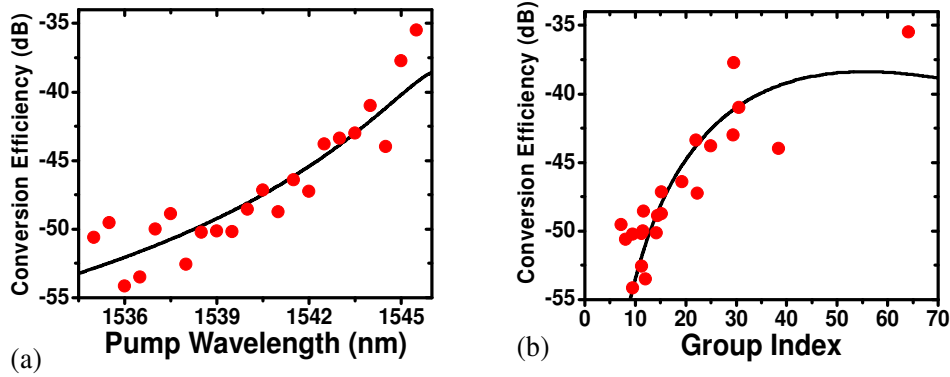


Fig. 5. (a) Four-wave mixing conversion efficiency dependence on pump wavelength ($|\lambda_{\text{signal}} - \lambda_{\text{pump}}| = 0.1\text{nm}$). (b) Conversion Efficiency dependence on n_g at λ_{pump} ; measurement (points), calculation (solid line).

As was discussed previously, the large dispersion of the PhCWG is responsible for the reduction in the bandwidth over which an appreciable idler power is measured as the pump wavelength gets closer to λ_c . The increasing values of $\beta_2(\lambda)$ and $\beta_4(\lambda)$ (See Fig. 4(a)) cause a larger phase mismatch between the interacting wavelengths within the propagation length of the PhCWG, resulting in the efficiency of conversion falling off more quickly with respect to pump and signal detuning. This phenomenon can be directly observed in the experimental data in Fig. 3(a) by observing the shrinking signal detuning bandwidth over which a measurable idler power is observed as the pump wavelength moves towards λ_c , giving the plot a distinctive triangular appearance. This limitation of the W1 waveguide has been reported previously [31] and can be mitigated by the introduction of regions of low-GVD into the waveguide dispersion by structural optimization [50,25].

To characterize the decrease in the FWM bandwidth as the pump is moved closer to λ_c the bandwidth of the measured conversion efficiency is plotted in Fig. 6(a). Due to the strong Fabry-Perot oscillations and limited resolution of the experimental data a conventional -3dB bandwidth could not be accurately gauged so we define the bandwidth as the total detuning range over which the conversion efficiency is within -10 dB of the maximum value for each pump wavelength. The same definition is applied to the simulated data to derive the bandwidth from the model. The measured results agree well with the model except for the last two measured pump wavelengths. This can be attributed to the imperfect match between the measured group index and the shifted numerically derived group index used for the model (illustrated in Fig. 1(a)) at these wavelengths. However, when the measured bandwidth is plotted with respect to group index, as it is in Fig. 6(b), this discrepancy is removed. The remaining deviations between experiment and model here are attributable to the finite signal wavelength step (0.1 nm) and the Fabry-Perot induced uncertainty in both the group index when using the phase shift method [51] and transmission when determining the -10 dB wavelengths.

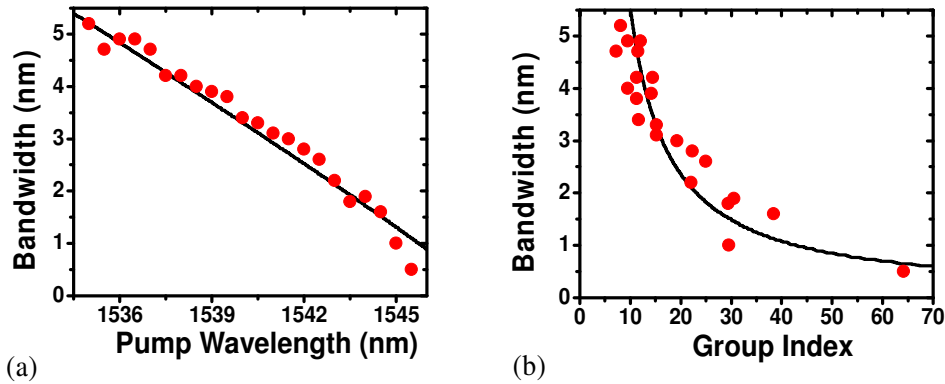


Fig. 6. The -10 -dB bandwidth dependence on (a) λ_{pump} and (b) n_g (at λ_{pump}); measurement (points), calculation (solid line).

It was stated previously that the model employed in this work uses a linear group index (n_g) scaling of the linear propagation loss: $\alpha^* = \alpha_0 (n_g/n_0)$, where α_0 , the minimum propagation loss, was 10 dB/cm. A linear scaling of loss with respect to group index was chosen because it was found to give the best fit to the experimental data. This fact is illustrated in Fig. 7 where the data presented in Fig. 5(b) is shown with the conversion efficiency of the model for different propagation loss n_g scaling factors with all other variables being equal. A number of recent experiments and theoretical investigations on the exact scaling of loss, both scattering loss due to fabrication disorder and loss caused by coupling to the backward propagating mode, with respect to group index in photonic crystal waveguides has provided a number of differing opinions on the subject [49,52–55], with several reports concluding that the fabrication disorder-induced loss in photonic crystal waveguides, like that of regular channel waveguides [56], scaling linearly with group index and that the loss from scattering of the forward propagating mode into the backward propagating mode scaling quadratically with group index. However, fabrication disorder can cause coherent scattering within and between unit cells of the waveguide along the direction of propagation [57]. In addition, there is a modification of the propagating Bloch mode shape with respect to frequency which has the effect of increasing the disorder sampling. These two factors have been used to suggest that the Beer-Lambert law and the simplistic view of relating group index scaling of loss fail for large group indices [58]. In regards to this experiment, since the majority of the data collected was in the n_g less than 40 regime, the dominant scaling of propagation loss observed in this experiment was linear.

One other possible source of experimental uncertainty with regard to the group index at λ_{pump} comes from the thermal shift of λ_c due to the presence of the pump beam. The thermal heating of the sample caused by the pump beam would cause a red-shift in the cutoff wavelength in contrast to the data presented in Fig. 1(a) which was collected at low optical powers. It is understandable that the waveguide would be more susceptible to the thermo-optic shifting of λ_c the larger the group index of the pump beam is, owing to the group index enhancement of optical intensity. However, due to the agreement between the calculated and measured bandwidth (see Fig. 6), which is directly dependant on the value of β_2 [59], we are confident that thermal shift of the group index value is minimal.

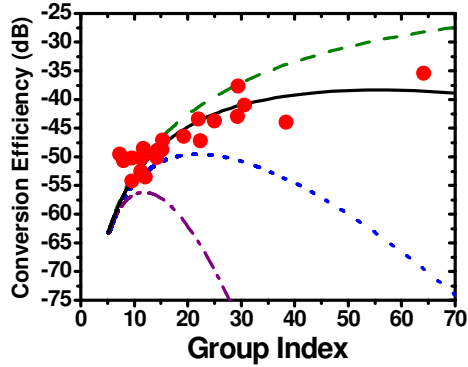


Fig. 7. Conversion Efficiency dependence on n_g at λ_{pump} for different propagation loss n_g scaling factors: $\alpha^* = \alpha_0 (n_g/n_0)^\delta$; $\delta = \sqrt{2}/2$ (dash), $\delta = 1$ (solid), $\delta = \sqrt{2}$ (dot), $\delta = 2$ (dash-dot), measurement (solid points).

5. Conclusion

We have experimentally investigated the group index enhancement of four-wave mixing in a W1 silicon photonic crystal waveguides. A 0.44 mm long waveguide exhibited a maximum conversion efficiency of -36 dB using a coupled pump power of 14 dBm. Over the wavelengths examined a group index enhancement of the third-order nonlinearity resulting in the conversion efficiency was to increase by over 12 dB from a $\Delta n_g \approx 55$. A corresponding decrease in the conversion efficiency bandwidth, from 5 nm to 0.5 nm, was also observed, which would severely limit the utility of the device in regard to most known applications of FWM in conventional silicon waveguide. Both of these experimental observations match well with a simple numerical model of four-wave mixing in photonic crystal waveguides which accounts for group index scaling of the propagation loss and nonlinear. The results presented here reinforce the slow-light nonlinear enhancement possible within silicon photonic crystal waveguides.

Acknowledgments

The authors acknowledge discussions with C. A. Husko, M.-C. Wu, and N. C. Panoiu. This work is supported by NSF (ECCS-0622069 and ECCS-0747787).